Journal of Computational Applied Mechanics 2021, 52(1): 332-349
DOI: 10.22059/jcamech.2021.315105.575

RESEARCH PAPER

Numerical Investigations of Two-Phase Flow on a Stepped Spillway under Various Conditions

Ehsan Parhizgar [1], Zafar Namazian [2,*]

[1] Department of Civil Engineering, Yasooj Branch, Islamic Azad University, Yasooj, Iran
[2] Department of Mechanical Engineering, Yasooj Branch, Islamic Azad University, Yasooj, Iran

Abstract
In this study, two-phase flow over a three dimensional stepped spillway was numerically investigated using a finite volume code in ansys-Fluent commercial software. The numerical results were validated against experimental data. Then, the effects of several parameters were evaluated on the structure of the flow over the concerned spillway. Based on the natural roughness, several roughness heights of 0.0001, 0.0005, and 0.001 m were considered on the spillway surface to investigate the flow structure. In the next step, several surfaces with different contact angles, including 80, 120, and 160°, were used. Finally, a passive control method, including simultaneous blowing and suction with different configurations, was applied to the steps of the spillway. The results revealed that a change in the surface roughness or contact angle and applying the control method could change the flow regime from skipping to nappe. Also, variations in the speed of falling water and energy loss were attributed to changes in the surface roughness and contact angle and implementation of the proposed control method.

Keywords: Stepped Spillway, Rough Surface, Hydrophobic to Superhydrophobic, Passive Control Method, Energy Dissipation, Discharge, Falling Velocity.

1. Introduction

A stepped spillway is a device placed along the river path that includes steps to contribute to reducing the loss of kinetic energy of the falling water. This removes or reduces the need for extra energy injection, such as a water body, at the end of the spillway of the downstream river. A stepped spillway is often used in steep places to transfer water, as well as dissipating energy and reducing erosion [1,2]. The stairs account for increasing the energy dissipation rate through the spillway and reducing the dimensions of the stilling basin. Nowadays, stepped spillways have been widely used in different parts of the world due to their extraordinary capacity to dissipate the energy flow and thus decrease the dimensions of the stilling basin, as well as controlling and reducing the vacuum phenomenon in the spillway. Also, using a stepped spillway can reduce the likelihood of cavitation over the spillway. In the past decades, researchers have done several studies to raise the performance of these spillways and have made great advancements. In general, researchers aim to decrease the downstream velocity by improving the performance of energy dissipation in the stepped spillway. Sorensen [3] has been one of the researchers in the field of the stepped spillway hydraulic.

* Corresponding author. e-mail: z.namazian@iauyasooj.ac.ir

Chamani et al. [4], Matos et al. [5], and Dong et al. [6] carried out many studies on the skimming flow regime. They also provided relationships to determine the amount of energy loss in this type of flow regime. Cheng et al. [7] numerically showed that the inception point (IP) of air entrainment could be observed, rapid air entrainment took place downstream of this point, and "white water" and eddies appeared in the corners of every step.

Wu et al. [8] analyzed the IP of a stepped spillway and reported an empirical equation based on their experimental data. Felder and Chanson [9] experimentally investigated the pooled and flat stepped spillways with various slopes. They concluded that the dissipation of energy in the pooled state was larger than that in the flat case with a smaller slope. Alghazali and Jasmin [10] obtained the position of IP in various configurations of stepped spillways. They derived twelve empirical relations for several stepped spillways configurations. Munta and Otun [11] performed forty experimental tests on some different stepped spillway configurations to obtain the relationship among IP, discharge, and chute angle. Also, the inception length increases as the unit discharge is elevated, where it diminishes by growing both stepped roughness height and chute angle. The pressure distributions on the spillway with various step configurations were evaluated by Daneshfaraz et al. [12]. They observed that the pressure values were larger for spillways with a smaller number of larger steps. Tabari and Tavakoli [13] investigated the effects of stepped spillway geometry on flow patterns and energy dissipation. The results revealed that energy dissipation decreases by increasing the flow discharge and the number of steps and reducing their height. Bai and Zhang [14] compared the pressure distribution of traditional and v-shaped stepped spillways and obtained the unique pressure distribution. Li et al. [15] examined steps with non-uniform heights at the bottom.

Their comparison between a curved spillways with/without steps showed that the steps balanced the partial centrifugal force on the curved part, causing the water depth of the cross-section to be evenly distributed and the other base plate to be covered with water. Li et al. [16] examined 45°-slope eight-stepped spillways with 8 different structures. They reported that the residual energy of the baffled-shifted rounded configuration was approximately eight and thirteen percent lower than that of the rounded and sharped configurations, respectively. The flow structures of a spillway approach channel at the guide wall of the Kamal-Saleh dam were studied by Parsaie et al. [17]. The results revealed that their geometry of the left wall caused instability in the flow pattern and formed the secondary and vortex flows at the beginning of the approach channel. Morovati and Eghbalzadeh [18] concluded that the inception point position had more influence on the nappe and transition flow regimes compared to the regime of the skimming flow, particularly at the heights of 9 and 15 cm. Li and Zhang [19] numerically studied the hydraulic characteristics of the skimming flow over pooled stepped spillway, concluding that the distribution of velocity in the direction of spanwise illustrated no significant difference among "fully pooled configuration", "fully pooled and two-sided pooled steps", and "two-sided pooled and central pooled steps". However, the velocity in two-sided pooled and central pooled steps was enhanced from the axial plane to the sidewalls; however, the peak of velocity in all states was approximately the same.

Ashoor and Riazi [20] numerically examined the non-uniform stepped spillways to evaluate the maximum energy dissipation. They reported that in semi-uniform stepped spillways with the ratio of 1:3 between the lengths of the successive steps, a vortex interference area occurred within the two adjacent cavities of the entire stepped chute that caused the energy dissipation to increase to 20%. Ghaderi et al [21] proposed a spillway with trapezoidal Labyrinth-shaped steps and showed that this type of spillway had better efficiency as it elevated the ratio of the spillway width to the total edge length. The effects of barrier height on the design of stepped spillway were experimentally investigated by Azman et al. [22].

Their results showed that as the height of the barrier was raised from 10 to 25 mm, the water flew down the steps faster at lower pressure, and the overall aeration efficiency was enhanced from 1.1 to 1.2%. Güven and Mahmood [23] numerically modeled the influence of the abrupt slope change on the flow features over a stepped spillway in the skimming flow regime. Their results indicated that near the slope change, the flow bulking, air entrainment, velocity distribution, and dynamic pressure are greatly affected. Ghaderi et al. [24] experimentally investigated the effective scouring parameters downstream of stepped spillways with various flow rates and step sizes. They showed that the enhancement in tailwater depth from 6.31 to 8.54 and then to 11.82 cm reduced the scouring depth by 18.56% and 11.42%, respectively.
Based on the literature, many studies have been conducted on the behavior of flow over the stepped spillways with various configurations, which have provided appropriate data to improve these structures. However, the effects of irregular roughnesses on the surface on the fluid flow structure have been less addressed. Therefore, one of the objectives of the present study is to investigate the presence of roughness of various heights on the spillway surface. Furthermore, surfaces with different contact angles are used to reduce the contact surface between water and solid. Also, a passive method [25,26] is implemented to enhance the performance of the stepped spillway. In this regard, a finite volume code in the two-phase state with the k-ω SST turbulence model [27-30] is employed.

2. Governing equations

According to the former conditions, the flow field was turbulent and assumed to be incompressible. Therefore, it does not need to solve the energy equation and the mass and momentum conservation equations are expressed as [29]:

$$\frac{\partial \bar{u}_j}{\partial x_j} = 0 \tag{1}$$

$$\frac{\partial \bar{u}_i}{\partial t} + \bar{u}_\iota \frac{\partial \bar{u}_i}{\partial x_j} = -\frac{1}{\rho}\frac{\partial P}{\partial x_i} + \upsilon \frac{\partial^2 \bar{u}_i}{\partial x_i \partial x_j} - \frac{\partial \overline{\dot{u}_\iota \dot{u}_j}}{\partial x_j} \tag{2}$$

Where, u is velocity field, t is flow time, P, υ, and x are pressure, viscosity, and the direction, respectively. In addition, in the present work, the VOF model was used to predict the liquid-air interface. The VOF model is a surface-tracking technique where the fluids share a single set of momentum equation, and the volume fraction of each fluid in each computational cell is tracked throughout the domain. The tracking of the interface between the phases is accomplished by the solution of a continuity equation for the volume fraction of one (or more) of the phases using the geometric reconstruction scheme. For the qth phase, this continuity equation has the following form:

$$\frac{\partial}{\partial_t}\left(\alpha_q \rho_q\right) + \nabla.\left(\alpha_q \rho_q u_q\right) = 0 \tag{3}$$

$$\frac{\partial(\rho u_i)}{\partial t} + \frac{\partial}{\partial x_j}\left(\rho u_j u_i\right) = -\frac{\partial p}{\partial x_j} + \frac{\partial}{\partial x_j}\left(\tau_{ij} + \tau_{t_{ij}}\right) + \rho g_i + F_{vol} \tag{4}$$

Where, α, g, and F_{vol} are phase volume fraction, gravity, and force due to surface tension, respectively. Also,

$$\rho = \alpha\rho_1 + (1-\alpha)\rho_2 \tag{5}$$

In which

$$K = -\frac{\partial n_i}{\partial x_i} = -\frac{\partial}{\partial x_i}\left(\frac{\frac{\partial \alpha}{\partial x_i}}{\left|\frac{\partial \alpha}{\partial x_i}\right|}\right) \tag{6}$$

It is worth noting that the following relationship is defined in each computational cell:

$$\sum_{q=1}^{n} \alpha_q = 1 \tag{7}$$

The volume source term of the momentum equation considering surface tension is presented in Eq. (8).

$$F_{vol} = \sigma_{ij} \frac{\rho \nabla . \left(\frac{\underbrace{\nabla \alpha_q}_{surface\ normal}}{|\nabla \alpha_q|} = \hat{n}\right)_i \nabla \alpha_i}{\frac{1}{2}(\rho_i + \rho_j)} \tag{8}$$

In this equation, σ is the surface tension and $\hat{n}$ is defined based on the divergence of the unit normal [31] and related to surface contact angle (θ_w) as follows:

$$\hat{n} = \widehat{n_w} \cos\theta_w + \hat{t}_w \sin\theta_w \tag{9}$$

The open channel flow [32] is characterized by an important dimensionless parameter called the Froude number (Fr).

$$Fr = \frac{V}{\sqrt{gy}} \tag{10}$$

In addition, the wave speed and total and static pressures are defined as:

$$V_w = V \pm \sqrt{gy} \tag{11}$$

$$\rho_. = \frac{1}{2}(\rho - \rho_.)V^2 + (\rho - \rho_.)|\vec{g}|\left(\hat{g}.\left(\vec{b} - \vec{a}\right)\right) \tag{12}$$

$$\rho_s = (\rho - \rho_.)|\vec{g}|\left(\left(\hat{g}.\hat{b}\right) + y_{local}\right) \tag{13}$$

Where y_{local} is the distance from the free surface to the reference position and defined as follows:

$$y_{local} = -(\vec{a}.\vec{g}) \tag{14}$$

Furthermore, the Reynolds averaged momentum equation of the VOF model is:

$$\frac{\partial \rho \overline{U_\iota}}{\partial t} + \frac{\partial}{\partial x_i}\left(\rho \overline{u_j}\,\overline{u_\iota}\right) = -\frac{\partial \bar{p}}{\partial x_i} + \frac{\partial \overline{\tau_{\iota J}}}{\partial x_j} + \overline{F_\iota} \tag{15}$$

$$\overline{\tau_{J\iota}} = \mu\left(\frac{\partial \bar{u}_i}{\partial x_j} + \frac{\partial \bar{u}_j}{\partial x_i}\right) - \rho\overline{\dot{u}_j\dot{u}_\iota} \tag{16}$$

F_i is the momentum source term. In Eq. (16), $-\rho\overline{\dot{u}_j\dot{u}_\iota}$ is the Reynolds stress term for which the *k-ω* shear-stress transport (k- *ω* SST) turbulence model is used that has proven to work well for wind turbine applications [33]. K-*ω* SST turbulence model is one of the most commonly utilized turbulence models. This model contains two additional transport equations to show the flow turbulent properties to account for history influences like convection and diffusion of the turbulent energy. The transport variables *k* and ω are used to calculate the energy in turbulence and the scale of turbulence, respectively [34]. The k-omega turbulence model can be utilized for boundary layer problems, where the formulation holds from the inner part through the viscous sub-layer until the walls. Hence, the k-ω SST turbulence model can be used in low-Re flow applications without additional damping functions. The SST formulation also switches to a k-ε turbulence model behavior in the free-stream, which avoids the k-ω problem to be very sensitive to the inlet free-stream turbulence properties.
The k-ω SST turbulence model is well known for its good behavior in adverse pressure gradients and separating flows [34]. It produces high turbulence levels in regions with large normal strain, e.g., stagnation regions and regions with strong acceleration. This effect is much less pronounced compared to a normal k-ε turbulence model. The k-omega shear stress transport turbulence model can fulfill the transport of the principal shear stress in adverse pressure gradient boundary-layers [34]. In the k-ω SST model, the turbulent kinetic energy, *k*, and the specific dissipation rate, *ω*, are obtained from the following transport equations [35]:

$$\frac{\partial}{\partial t}(\rho k) + \frac{\partial}{\partial x_i}(\rho k u_i) = \frac{\partial}{\partial x_j}\left(\Gamma_k \frac{\partial k}{\partial x_j}\right) + G_k - Y_k \tag{17}$$

$$\frac{\partial}{\partial t}(\rho \omega) + \frac{\partial}{\partial x_i}(\rho \omega u_i) = \frac{\partial}{\partial x_j}\left(\Gamma_\omega \frac{\partial \omega}{\partial x_j}\right) + G_w - Y_w + D_w \tag{18}$$

Where, G_k and G_ω stand the generation of turbulence kinetic energy (k) and ω as well as Y_k, and Y_ω are the Dissipation of k and ω.

3.Computational domain and grid study

Figure 1 indicates the three dimensional computational domain used in this study. The profile spillway crown is y/H=3.66326(x/H)1.85 where x, y, and H are the horizontal, vertical components, and height (78.9 cm) from the toe of the flow of water on the spillway, and the design head was 9.7 cm. Below the contact point, the spillway profile had a Chute slope of 1Vertical:0.75Horizontal, which was connected to the paw by a 28cm arch. From the fifth step on, the dimensions of the stairs were uniform and equal to 6×4.5 cm. The height to width ratio of the first 5 steps varied so that the tip of the stairs became tangential to the standard profile. The heights of the first 5 steps were 4, 2.2, 3, 4, and 5 cm, respectively. The spillway had a width of 30 cm, and the length of the channel with an approaching flow was 3 m. The downstream slope of the claw was zero, and the guide and downstream channels of the

spillway claw had the same width of 30 cm. Also, based on Ref. [33], the flow rate was set at 0.02 m3.s-1. Moreover, according to Fig. 1a, velocity inlet, pressure outlet, and no-slip boundary conditions were considered for inlet, outlet, and wall, respectively.

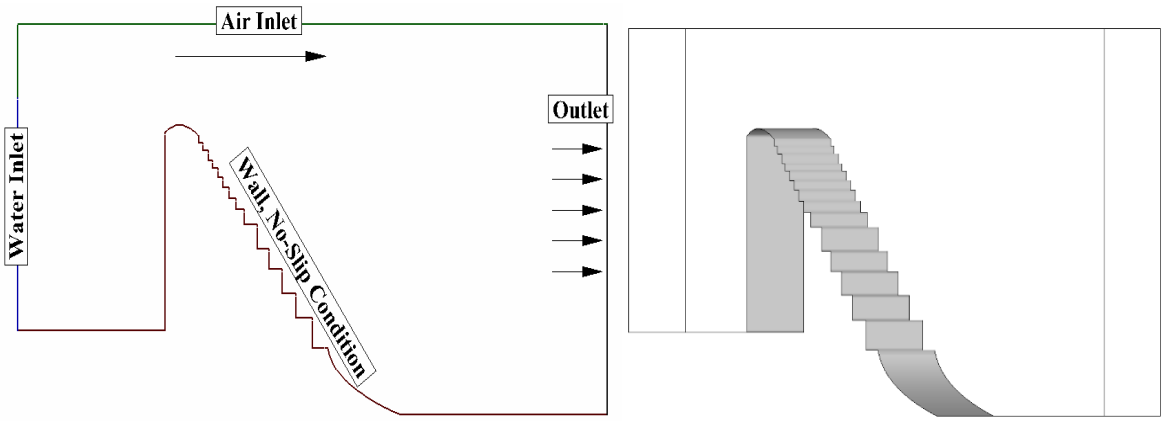

a b

Fig. 1. a) Boundary conditions and b) computational domain

For the grid independency study, three cell configurations with 10^5, 3×10^5, and 6×10^5cells were used. As can be observed in Fig. 2a, the distribution of velocity along the flow on the stairs was almost the same for grids with more than 3×10^5 cells. This cell configuration led to a reduction in the computational time up to half of the time for the grid with 6×10^5 cells. Furthermore, to decrease the solution fluctuations, a stable solution with a residual of less than 10^{-6} was obtained using this cell structure. Figure 2b shows a schematic of the grid with structured cells in the present work. Additionally, in the areas far from the spillway, the grids gradually become larger, but the aspect ratio of the cells did not exceed 3 in most areas of the computational field. Also, in the calculations and simulations performed in the present work, the residual values for all parameters were less than 10^{-4}.

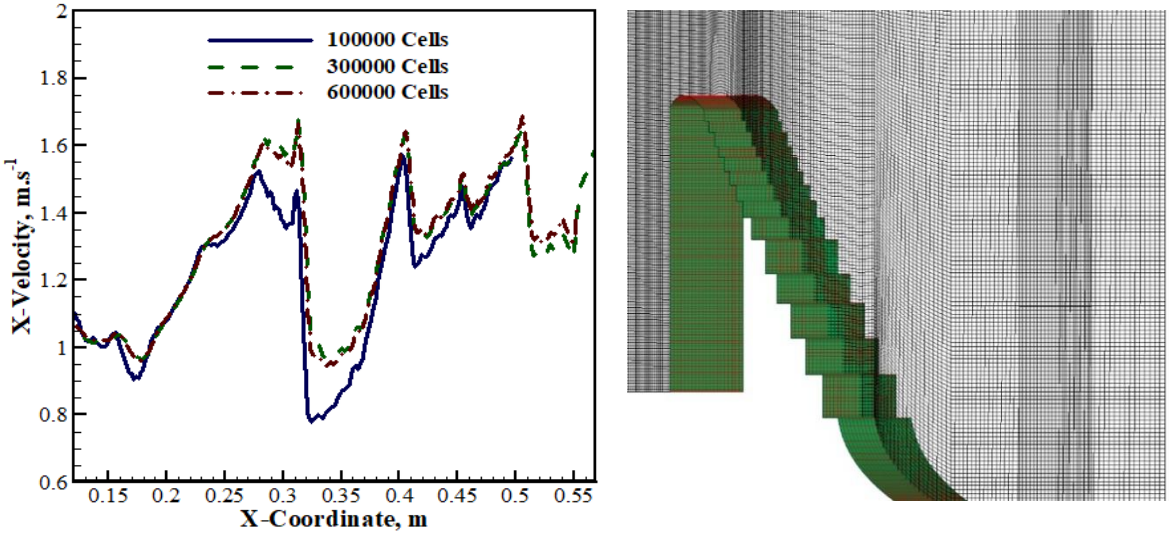

a b

Fig. 2. a) Grid study, b) the cell sample configuration

4. Results and discussions

4.1.Validation

In this section the numerical results are compared with the available experimental data [36], see Fig. 3. based on the work with [36], The water flows with the rate of 0.02 $m^3.s^{-1}$ over a spillway with the crown by $y=3.66326x^{1.85}$ profile, Chute slope of 1V:0.75H, and with different height step from 2 to 5 cm as mentioned previously. As can be observed, the present two-phase numerical method and the k-ω SST turbulence model (due to its ability to predict recirculation and separation flows in steps) predicted the water height with R-square [37] of more than 97% compared to Ref. [36]. After validating the numerical method, several effective parameters were investigated.

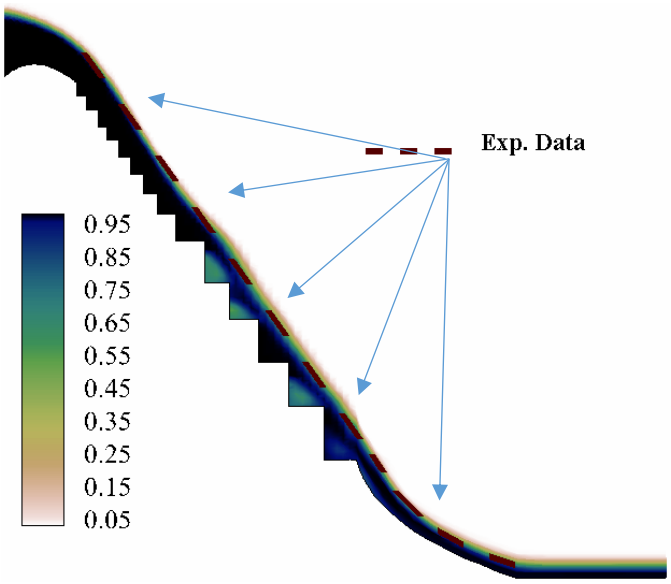

Fig. 3. Validation of the present finite volume code

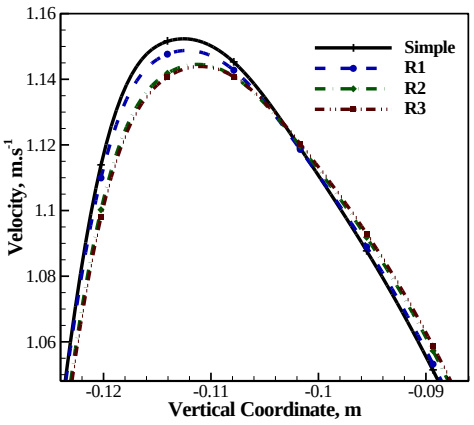

20 mm

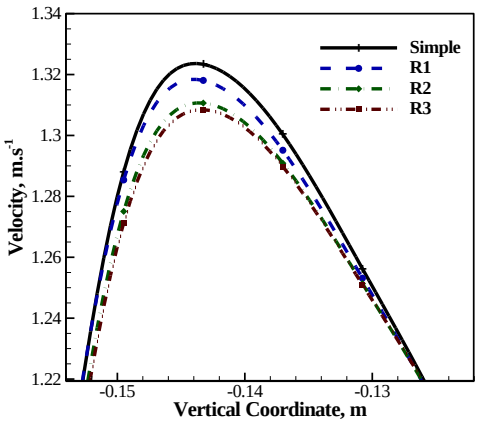

23 mm

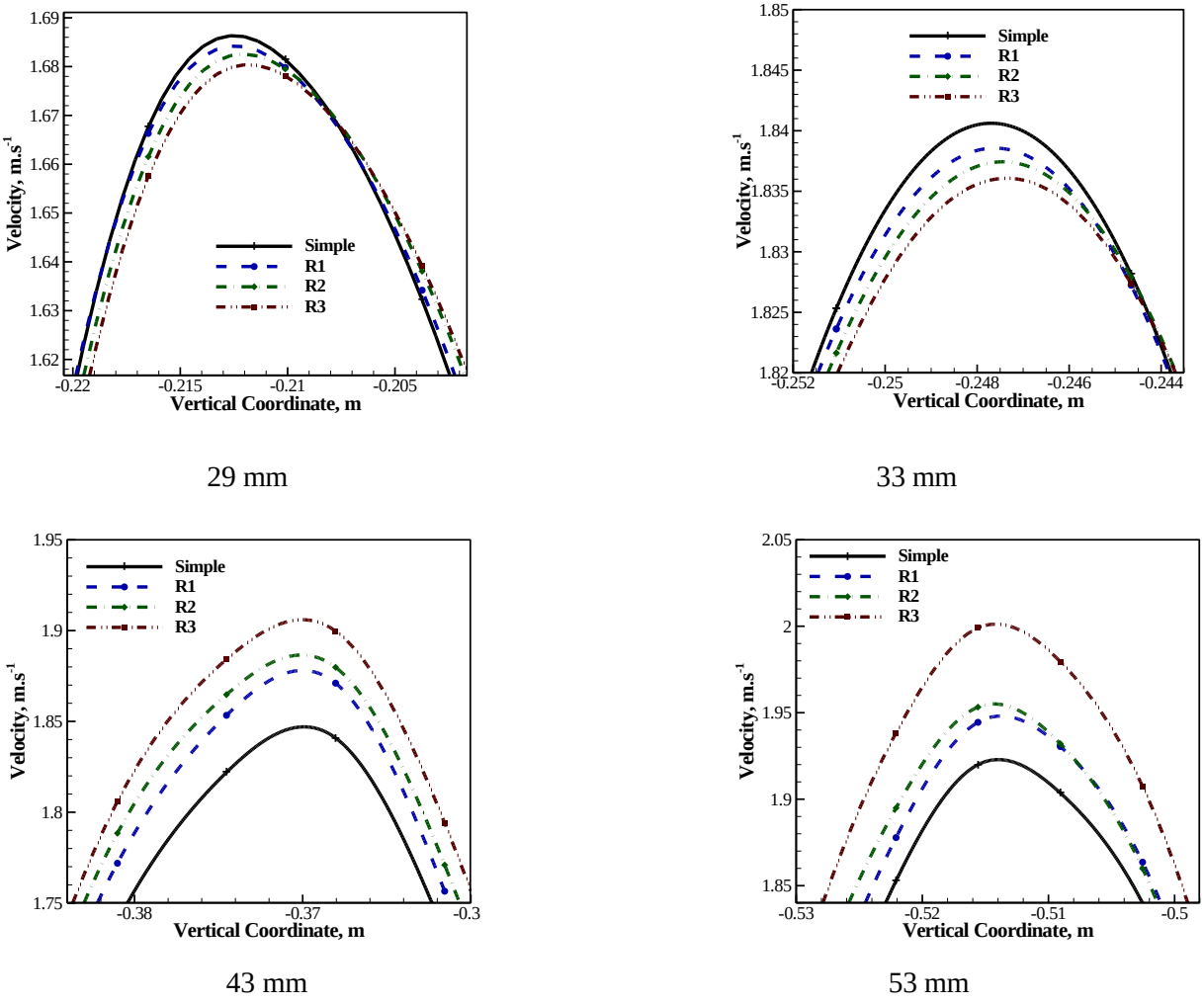

Fig. 4. Vertical velocity over smooth and rough spillways at various distances

4.2.Effects of Roughness

Given that no surface can be completely smooth, this section examines the effects of roughness on spillway stairs on the flow behavior. In this regard, three roughness heights of 0.0001, 0.0005, and 0.001 meters were employed. Figure 4 indicates the vertical velocity distribution at different distances from the spillway crown, including 20, 23, 29, 33, 43, and 53 mm. These distances were determined such that the flow characteristics could be observed at the center of the stairs. Also, close to the spillway crown and before its middle part, the falling velocity was higher for the smooth state compared to rough spillways. Also, as the height of the roughness increased, the velocity of the water flow decreased at distances of up to 33 mm from the spillway crown. However, as the flow approached the spillway floor, the flow behavior changed, i.e., raising the roughness height increased the rate of water falling. This is because the turbulence level increased and the water flow was shifted to the nappe regime by increasing roughness height (Fig. 5).

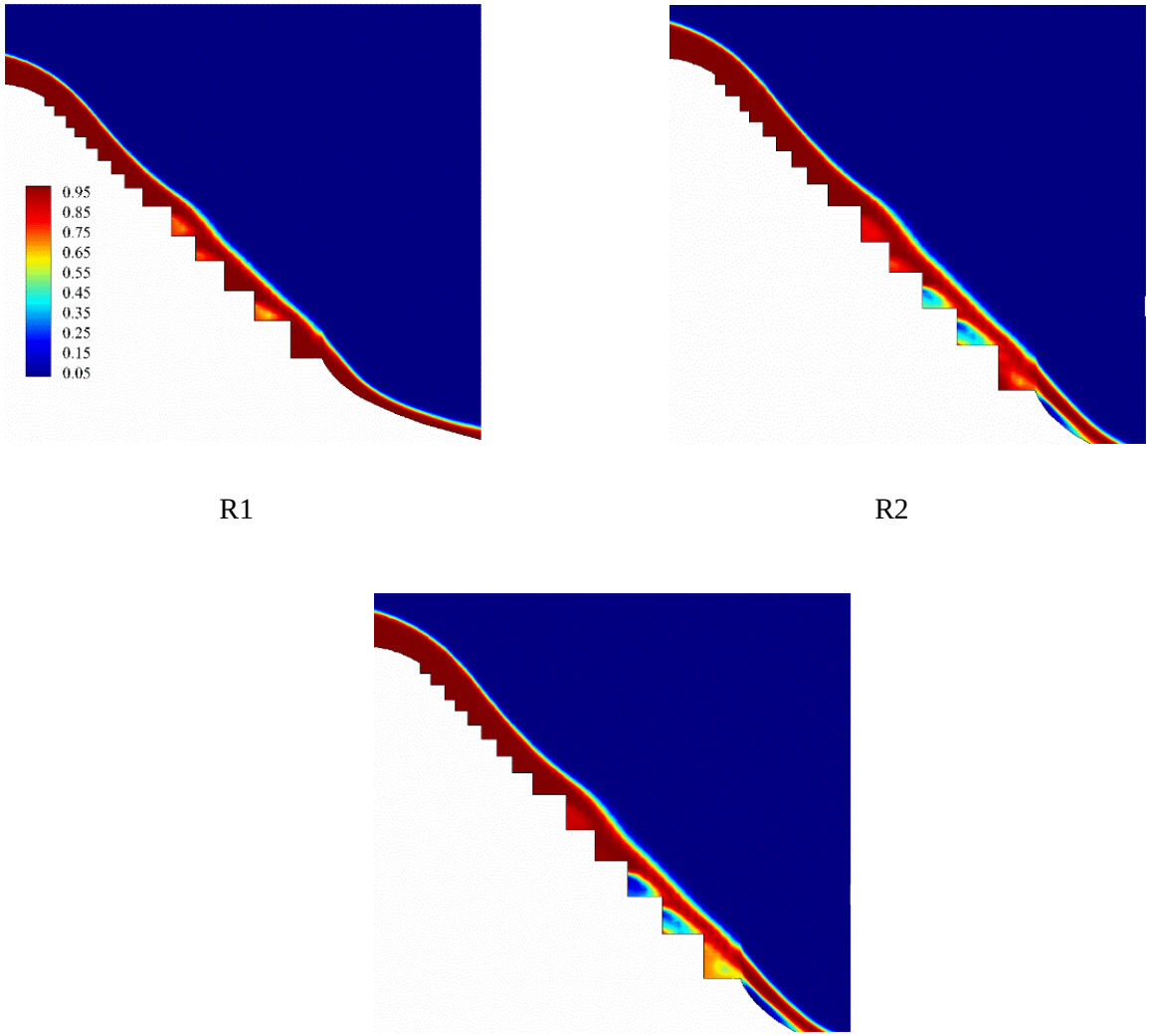

Fig. 5. Flow over the rough spillway

In this regime, the water flow is more in contact with the air than the solid surface. Therefore, the effects of water viscosity were reduced and as a result, the flow was transferred downstream more quickly at further distances away from the spillway crown. The increase in the length of the separation zone can be observed in Fig. 6. As shown, increasing the roughness height at all distances enlarged the length of the flow separation area. This is because of the increasing the level of turbulence intensity with growth in roughness height. In general this seapration increased the loss of flow energy and also the discharge factor. Also, at a distance of 57 mm from the spillway crown, there was no flow separation for the smooth and rough case (R1), i.e., in the downstream areas of the spillway, the roughness had no noticeable effect on the recirculation flow behavior. Furthermore, in R3, there was a minimum value for the flow velocity since wall roughness enhanced turbulent boundary layer skin friction and produced thicker boundary layers [38].

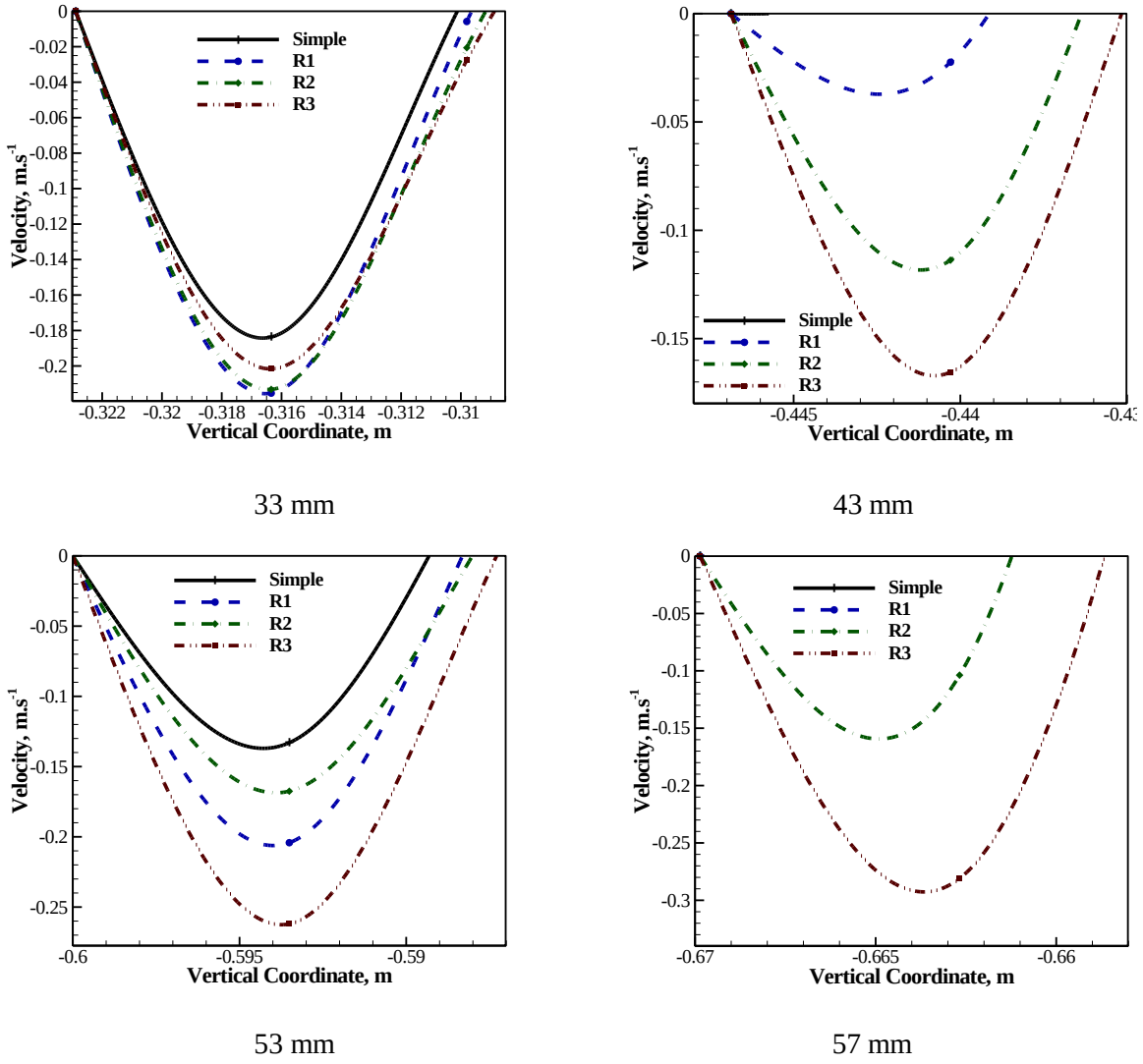

Fig. 6. Separation area length at various locations in smooth and rough spillways

4.3.Hydrophilic,hydrophobic, and superhydrophobic surfaces

In this section, surfaces with different contact angles such as 80° (hydrophilic surface), 120° (hydrophobic surface), and 160° (superhydrophobic) [39] were investigated. A surface with a high contact angle reduced the water contact area with a solid surface. This contact reduction undermined the role of fluid viscosity and decreased the adhesion between the surface and the fluid flow. A decrease in viscosity raised the Reynolds number of the flow, thereby increasing the flow separation and changing the flow regime from skimming to transition, followed by nappe flow. Figure 7 indicates the length of the flow separation area for spillway with different contact angles. It should be noted that using the surface with a high contact angle led to a reduction in skin friction due to the reduction of the level of surface contact of fluid flow and solid surface. In addition, as mentioned above, as the contact angle increased, the Reynolds number was elevated, growing turbulence intensity as the main factor in controlling the positive pressure gradient.

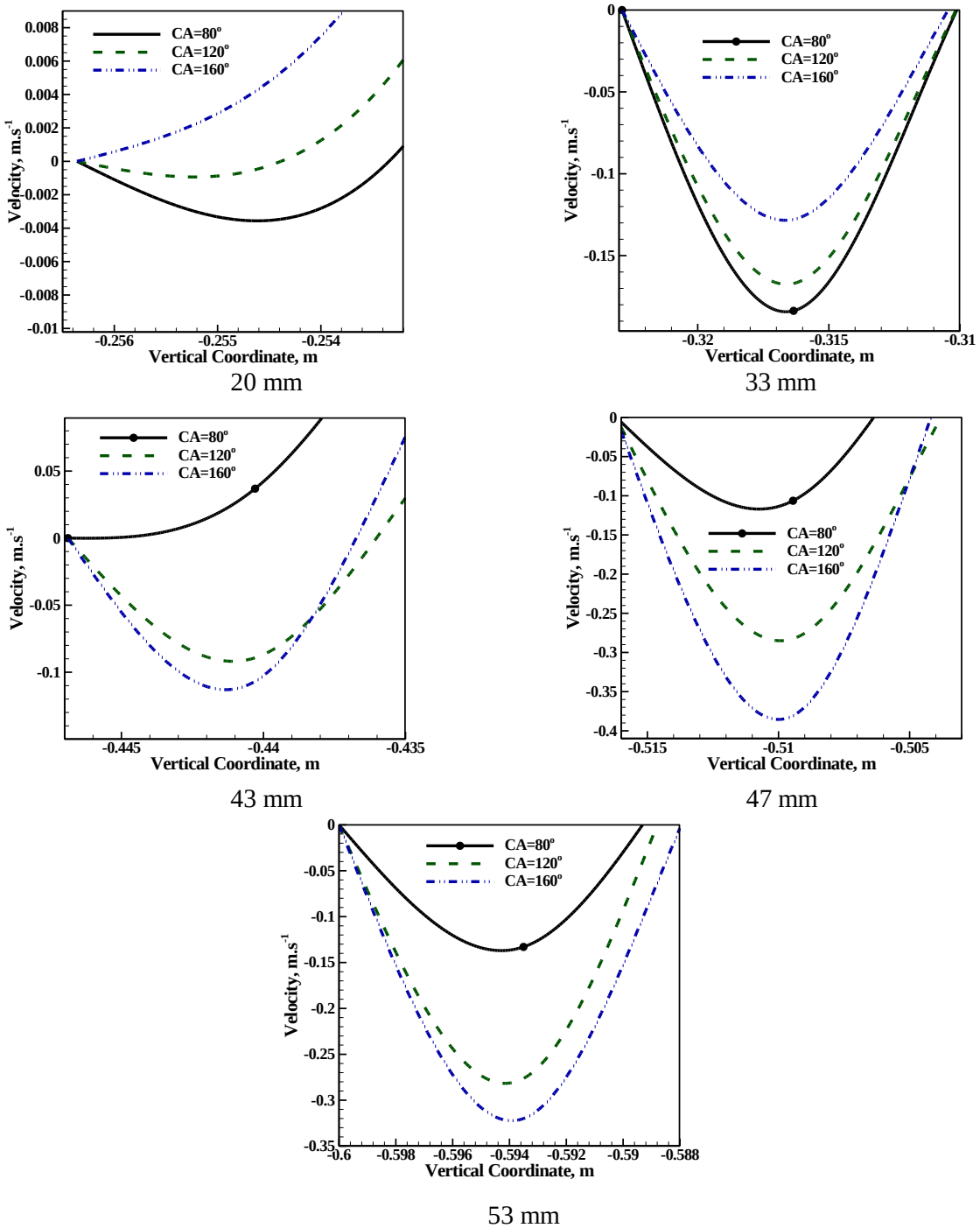

Fig. 7. Effects of contact angle on the length of the separation area

As can be observed, a change in the contact angle varied the characteristics of the separation and recirculation flows on the steps. Thus, up to a distance of 33 mm from the spillway crown, the flow separation area for the superhydrophobic surface was smaller than that of the hydrophilic surface. Similar to the previous section, the superhydrophobic surface increased the flow separation area length and the discharge coefficient as well.

4.4.Effects of Passive Control Method

In this section, the effects of flow control methods [26,40] were investigated on the behavior of the fluid flow over the spillways. The presence of blowing and suction as active control methods caused a change in the structure of the boundary layer and Tollmien–Schlichting waves. Since the implementation of active control methods requires energy expenditure, here, the passive artificial blowing and suction methods were developed for the spillway steps using natural flow characteristics. According to Fig. 8, three different cases (C1-C3) were used to perform this study. Every other one step for C1, every other 2 steps for C2, every other four and five steps for C3 were considered within a separate path. In this regard, the water flow at the top of the separate path was led to the main path using gravity; accelerated due to the gravitational force and blown down as an artificial jet to the downstream steps.

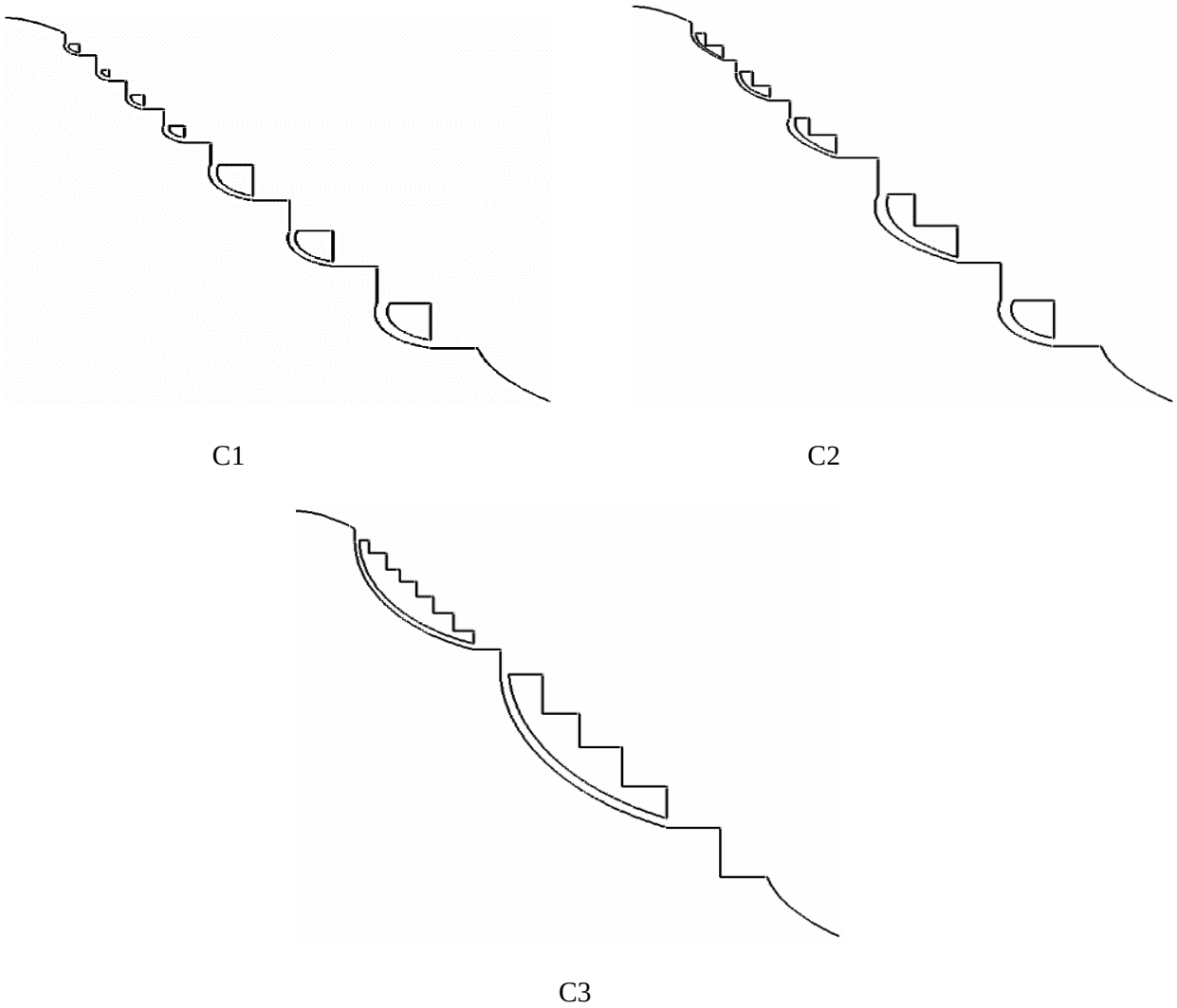

Fig. 8. Schematic of the patterns of passive control methods

Figure 9 indicates the phase contour for the three mentioned states. As can be seen, there were nappe regimes in C2, which increased the rate of water falling. Also, for C3, in the spillway upstream, the flow was oriented between the transition and nappe regimes; therefore, the water falling velocity was higher than that in C1 and main (without control method) cases. In C1, in most areas, the flow varied between transition and skimming regimes and had the lowest velocity. Based on the above explanations, it can be said that C1 reduced energy loss and C2 increased flow velocity and energy loss. Furthermore, Fig. 10 depicts the velocity distribution at different distances from the spillway crown. As can be observed at all distances, a higher falling velocity was achieved for C2; accordingly,

it can be stated that the use of this passive control method improved the spillway discharge coefficient and energy dissipation on average. This is because this passive control method caused an increase in the momentum of the fluid flow and, thus, the flow behavior near the steps changed. Moreover, the proposed control method yielded an increase in the instability of the flow pattern, as well as provoking the secondary flow and vortex flow. By comparing the results, these phenomena were greater for C2 than C1 and C3.

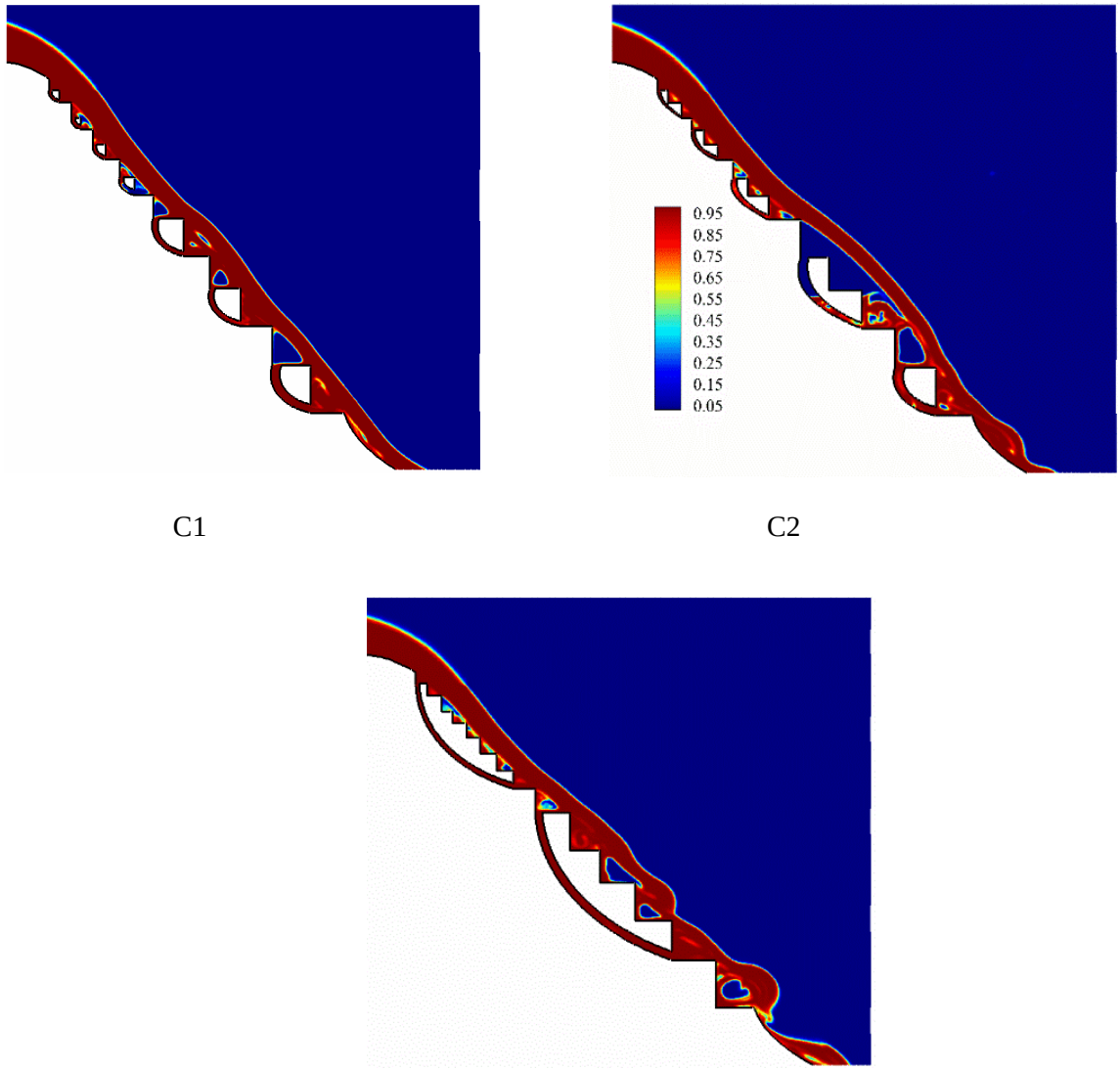

Fig. 9. Two-phase distribution over the spillways in the three cases

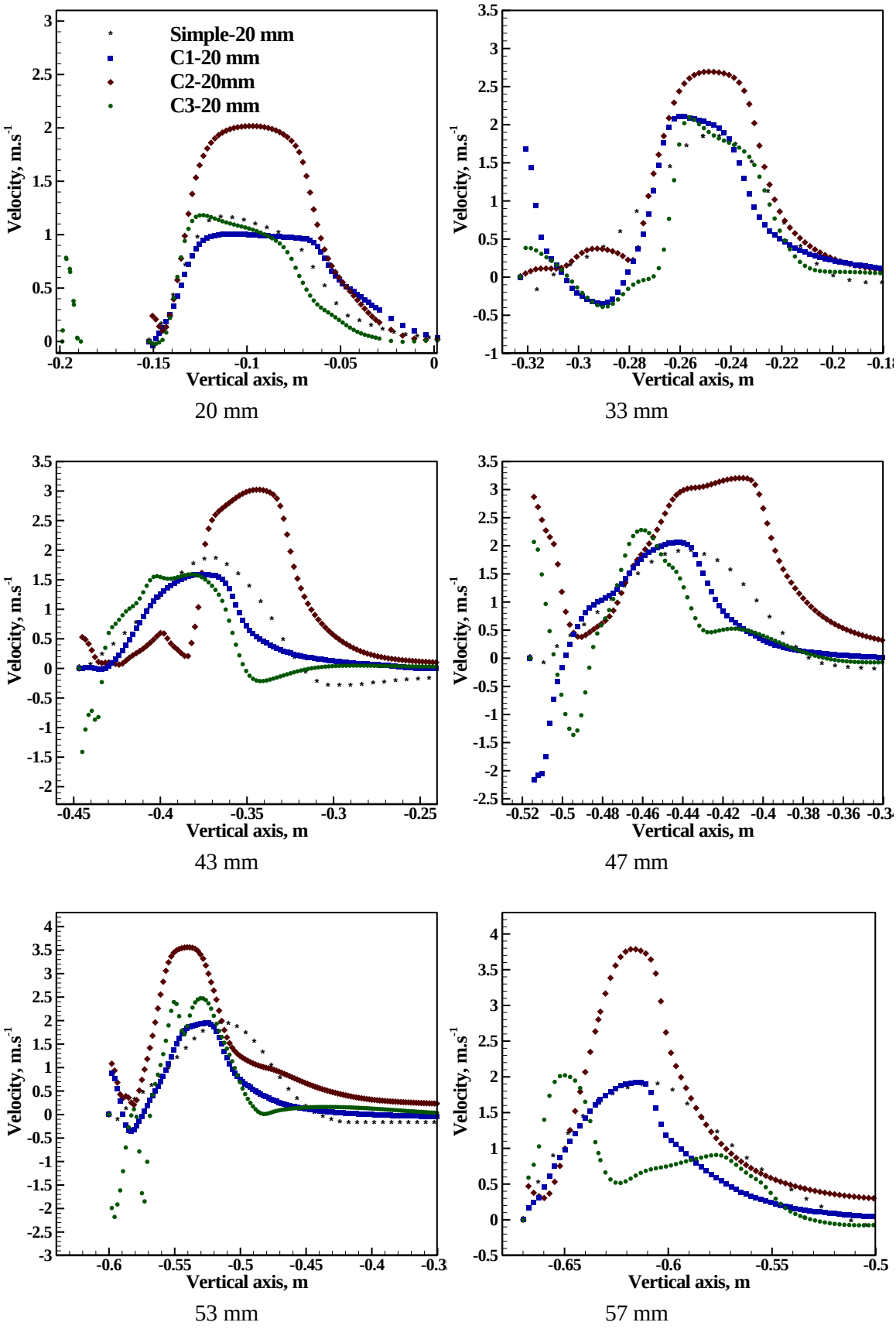

Fig. 10. Vertical velocity distribution at various distances from the spillway crown

5.Conclusion

In the present study, a 3D investigation of the behavior of the flow over a stepped spillway was conducted using a two-phase finite volume code. First, the results were compared with the experimental data, suggesting the high accuracy of the numerical method used in this study. After validating the results, several effective parameters (e.g., surface roughness and contact angle) and a passive control method were used. The obtained results can be summarized as follows:

- As the surface roughness height increased, the flow turbulence grew, fluid flow was transferred to the nappe regime, and the flow was transferred to the downstream more quickly at further distances away from the spillway crown. Furthermore, an increase in the surface roughness height led to the enlargement of the separation region. Finally, the presence of roughness increased discharge factor and energy loss.
- The presence of a surface with a high contact angle caused a decrease in the contact of water flow with the solid surface, thereby undermining the role of fluid viscosity. Therefore, the Reynolds number of the flow was raised and, in turn, flow separation was intensified. Thus, the flow regime was transferred from skimming to transition and then to the nappe regime. Moreover, the results revealed that by getting away from the spillway crown, the surface became more hydrophobic and a large area of flow separation took place on the steps. Finally, it can be concluded the hydrophobic surface increased the flow separation and discharge factor.
- Applying the proposed passive control method caused a change in the flow regime. In Case 2, the nappe regime was created in some areas that led to an increase in the falling water velocity. Also, Case 3 was oriented between transition and nappe regime in upstream regions. Thus, the falling water flow in Case 3 was more rapid (i.e., higher discharge factor) compared to C1 and the main case. Further, the implementation of the proposed control method caused instabilities in the flow pattern and provoked secondary and vortex flows, which were more considerable for C2 compared to C1 and C3.

References

[1] Liao L., An R., Li J., Yi W., Liu X., Meng W., Zhu L., Hydraulic characteristics of stepped spillway dropshafts for urban deep tunnel drainage systems: the case study of Chengdu city, *Water Science and Technology* 80 (8): 1538-1548. doi:10.2166/wst.2019.405, 2019.
[2] Fadaei Kermani E., Barani GA., Ghaeini-Hessaroeyeh M., Prediction of cavitation damage on spillway using K-nearest neighbor modeling, Water Science and Technology 71 (3):347-352, doi: 10.2166/wst.2014.495, 2014
[3] Sorensen Robert M., Stepped Spillway Hydraulic Model Investigation, *Journal of Hydraulic Engineering* 111 (12): 1461-1472, doi:10.1061/(ASCE)0733-9429(1985)111:12(1461), 1985.
[4] Chamani MR., Rajaratnam N., Characteristics of Skimming Flow over Stepped Spillways. *Journal of Hydraulic Engineering* 125 (4): 361-368, doi:10.1061/(ASCE)0733-9429, 1999,125:4(361), 1999.
[5] Matos J., Sanchez M., Quintela A., Dolz J. , Characteristic depth and pressure profiles in skimming flow over stepped spillways, *Proceedings of the 29th IAHR congress*, Graz, Austria, 1999.
[6] Dong Z-y., Lee JH-w., Numerical simulation of skimming flow over mild stepped channel*, *Journal of Hydrodynamics*,Ser B 18 (3): 367-371, doi:https://doi.org/10.1016/S1001-6058(06)60018-8, 2006.
[7] Cheng X., Chen Y., Luo L., Numerical simulation of air-water two-phase flow over stepped spillways, Science in China Series E: *Technological Sciences* 49 (6): 674-684, doi:10.1007/s10288-006-2029-2, 2006.
[8] Wu J-h., Zhang B., Ma F., Inception point of air entrainment over stepped spillways, *Journal of Hydrodynamics* 25 (1):91-96, doi:10.1016/S1001-6058(13)60342-X, 2013.
[9] Felder S., Chanson H., Air entrainment and energy dissipation on porous pooled stepped spillways, IWLHS, *International Workshop on Hydraulic Design of Low-Head Structures*, Aachen - Bung & Pagliara, pp 87-97, 2013.
[10] Alghazali M., Jasim SM., Location of air inception point for different configurations of stepped spillways, *International Journal of Civil Engineering and Technology* 5 (4): 82–90, 2014.
[11] Munta S., Otun J., Study of the Inception Length of Flow over Stepped Spillway Models, *Nigerian Journal of Technology* 33 (2): 176-183, 2014.
[12] Daneshfaraz R., Joudi AR., Ghahramanzadeh A., Ghaderi A., Investigation of flow pressure distribution over a stepped spillway, *Advances and Applications in Fluid Mechanics* 19 (4): 811-828, doi:10.17654/FM019040811, 2016.
[13] Mohammad Rezapour Tabari M., Tavakoli S., Effects of Stepped Spillway Geometry on Flow Pattern and Energy Dissipation, *Arabian Journal for Science and Engineering* 41 (4): 1215-1224,. doi:10.1007/s13369-015-1874-8, 2016.
[14] Bai Z., Zhang J., Comparison of Different Turbulence Models for Numerical Simulation of Pressure Distribution in V-Shaped Stepped Spillway, *Mathematical Problems in Engineering* 2017:3537026, doi:10.1155/2017/3537026, 2017.
[15] Li D., Yang Q., Ma X., Dai G., Case study on application of the step with non-uniform heights at the bottom using a numerical and experimental model, *Water (Switzerland)* 10 (12) , doi:10.3390/w10121762, 2018.
[16] Li S., Zhang J., Xu W., Numerical investigation of air–water flow properties over steep flat and pooled stepped spillways, *Journal of Hydraulic Research* 56 (1): 1-14. doi:10.1080/00221686.2017.1286393, 2018.

[17] Parsaie A., Moradinejad A., Haghiabi AH., Numerical modeling of flow pattern in spillway approach channel, *Jordan Journal of Civil Engineering* 12 (1): 1-9, 2018.
[18] Morovati K., Eghbalzadeh A., Study of inception point, void fraction and pressure over pooled stepped spillways using Flow-3D, *International Journal of Numerical Methods for Heat and Fluid Flow* 28 (4): 982-998, doi:10.1108/HFF-03-2017-0112, 2018.
[19] Li S., Zhang J., Numerical Investigation on the Hydraulic Properties of the Skimming Flow over Pooled Stepped Spillway, *Water* 10 (10):1478, 2018.
[20] Ashoor A., Riazi A., Stepped spillways and energy dissipation: A non-uniform step length approach, *Applied Sciences (Switzerland)* 9 (23) , doi:10.3390/app9235071, 2019.
[21] Ghaderi A., Abbasi S., Abraham J., Azamathulla HM., Efficiency of Trapezoidal Labyrinth Shaped stepped spillways, *Flow Measurement and Instrumentation* 72:101711, doi:https://doi.org/10.1016/j.flowmeasinst.2020.101711, 2020.
[22] Azman A., Ng FC, Zawawi MH., Abas A., Rozainy M. A. Z MR., Abustan I., Adlan MN., Tam WL., Effect of Barrier Height on the Design of Stepped Spillway Using Smoothed Particle Hydrodynamics and Particle Image Velocimetry, *KSCE Journal of Civil Engineering* 24 (2): 451-470, doi:10.1007/s12205-020-1605-x, 2020.
[23] Güven A., Mahmood AH., Numerical investigation of flow characteristics over stepped spillways, *Water Supply in press*, doi:10.2166/ws.2020.283, 2020.
[24] Ghaderi A., Daneshfaraz R., Torabi M., Abraham J., Azamathulla HM., Experimental investigation on effective scouring parameters downstream from stepped spillways, *Water Supply* 20 (5): 1988-1998. doi:10.2166/ws, 2020.113, 2020.
[25] Sotoudeh F., Pourabidi R., Mousavi SM., Goshtasbi-Rad E., Jeung I-S., Hybrid passive-active control method of a swept shock wave-supersonic wake interaction, *Acta Astronautica* 160:509-518, doi:https://doi.org/10.1016/j.actaastro.2019.02.023, 2019.
[26] Mousavi SM., Kamali R., Sotoudeh F., Karimi N., Khojasteh D., Large eddy simulation of pseudo shock structure in a convergent–long divergent duct, *Computers & Mathematics with Applications*, doi:https://doi.org/10.1016/j.camwa.2019.10.017, 2019.
[27] Mousavi SM., Kamali R., Mathematical Modeling of the Vortex Shedding Structure and Sound Pressure Level of a Large Wind Turbine Tower, *International Journal of Applied Mechanics* 12 (06):2050070, doi:10.1142/S1758825120500702, 2020.
[28] Sotoudeh F., Kamali R., Mousavi SM., Field tests and numerical modeling of INVELOX wind turbine application in low wind speed region, *Energy* 181:745-759, doi:https://doi.org/10.1016/j.energy.2019.05.186, 2019.
[29] Binesh AR., Mousavi SM., Kamali R., Effect of temperature-dependency of Newtonian and non-Newtonian fluid properties on the dynamics of droplet impinging on hot surfaces, *International Journal of Modern Physics C* 26 (09):1550106, doi:10.1142/S0129183115501065, 2015.
[30] Mousavi SM., Kamali R., Experimental and numerical investigation of a new active control method to suppression of vortex shedding and reduction of sound pressure level of a circular cylinder, *Aerospace Science and Technology* 103:105907, doi:https://doi.org/10.1016/j.ast.2020.105907, 2020.
[31] Brackbill JU., Kothe DB., Zemach C., A continuum method for modeling surface tension, *Journal of Computational Physics* 100 (2):335-354, doi:https://doi.org/10.1016/0021-9991(92)90240-Y, 1992.
[32] Chaudhry MH., Open-channel flow, *Springer Science & Business Media*, 2007.
[33] Chitsomboon T. , and C. Thamthæ, Adjustment of k-w SST turbulence model for an improved prediction of stalls on wind turbine blades, *World Renewable Energy Congress-Sweden, Linköping University Electronic Press*, 2011.

[34] Menter F., Zonal Two Equation k-w Turbulence Models For Aerodynamic Flows, 23rd Fluid Dynamics, Plasmadynamics, and Lasers Conference, *American Institute of Aeronautics and Astronautics*, 1993.
[35] Menter F., "Two-equation eddy-viscosity turbulence models for engineering applications," *AIAA journal* 32(8): 1598-1605, 1994.
[36] Chen Q., Dai G., Liu H., Volume of Fluid Model for Turbulence Numerical Simulation of Stepped Spillway Overflow, *Journal of Hydraulic Engineering* 128 (7): 683-688, doi:10.1061/(ASCE)0733-9429(2002)128:7(683), 2002.
[37] Mousavi SM., Roohi E., Large eddy simulation of shock train in a convergent–divergent nozzle, *International Journal of Modern Physics* C 25 (04):1450003, doi:10.1142/S012918311450003X, 2013.
[38] Song S., Eaton J., The effects of wall roughness on the separated flow over a smoothly contoured ramp, *Experiments in Fluids* 33 (1): 38-46, doi:10.1007/s00348-002-0411-1, 2002.
[39] Khojasteh D., Manshadi MKD., Mousavi SM., Sotoudeh F., Kamali R., Bordbar A., Electrically modulated droplet impingement onto hydrophilic and (super)hydrophobic solid surfaces, *Journal of the Brazilian Society of Mechanical Sciences and Engineering* 42 (4): 153, doi:10.1007/s40430-020-2241-6, 2020.
[40] Kamali R., Mousavi SM., Khojasteh D., Three-Dimensional Passive and Active Control Methods of Shock Wave Train Physics in a Duct, *International Journal of Applied Mechanics* 08 (04):1650047, doi:10.1142/S1758825116500472, 2016.